AD-A082 242 LOCKHEED MISSILES AND SPACE CO INC PALO ALTO CA PALO --ETC F/G 3/2
SOLAR MAGNETIC FIELD STUDIES (PHOTON COUNTER).(U)
OCT 79 L N MERTZ F19628-79-C-0183
UNCLASSIFIED LMSC/D682393 AFGL-TR-79-0240 NL

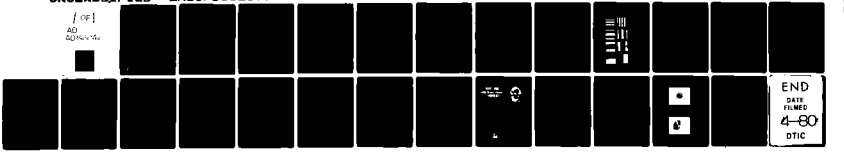

AFGL-TR-79-0240

SOLAR MAGNETIC FIELD STUDIES (PHOTON COUNTER)

L. Mertz
Lockheed Palo Alto Research Laboratory
3251 Hanover Street
Palo Alto, California 94304

October 1979

Final Report for Period August 1979 - September 1979

Approved for public release; distributions unlimited

AIR FORCE GEOPHYSICS LABORATORY
AIR FORCE SYSTEMS COMMAND
UNITED STATES AIR FORCE
HANSCOM AFB, MASSACHUSETTS 01731

UNCLASSIFIED

SECURITY CLASSIFICATION OF THIS PAGE (When Data Entered)

REPORT DOCUMENTATION PAGE	READ INSTRUCTIONS BEFORE COMPLETING FORM
1. REPORT NUMBER: AFGL-TR-79-0240	2. GOVT ACCESSION NO.	3. RECIPIENT'S CATALOG NUMBER
4. TITLE (and Subtitle): SOLAR MAGNETIC FIELD STUDIES (PHOTON COUNTER)	5. TYPE OF REPORT & PERIOD COVERED: Final 8-15-79 to 9-30-79
	6. PERFORMING ORG. REPORT NUMBER: LMSC/D682393
7. AUTHOR(s): L. Mertz	8. CONTRACT OR GRANT NUMBER(s): F19628-79-C-0183
9. PERFORMING ORGANIZATION NAME AND ADDRESS: Lockheed Palo Alto Research Laboratory, 3251 Hanover Street, Palo Alto, California 94304	10. PROGRAM ELEMENT, PROJECT, TASK AREA & WORK UNIT NUMBERS: 61102F, 2311G3AL
11. CONTROLLING OFFICE NAME AND ADDRESS: Air Force Geophysics Laboratory, Hanscom AFB, Massachusetts 01731, Monitor/Donald F. Neidig/PHS	12. REPORT DATE: October 1979
	13. NUMBER OF PAGES
14. MONITORING AGENCY NAME & ADDRESS (if different from Controlling Office)	15. SECURITY CLASS. (of this report): UNCLASSIFIED
	15a. DECLASSIFICATION/DOWNGRADING SCHEDULE

16. DISTRIBUTION STATEMENT (of this Report)

Approved for public release; distribution unlimited.

17. DISTRIBUTION STATEMENT (of the abstract entered in Block 20, if different from Report)

18. SUPPLEMENTARY NOTES

19. KEY WORDS (Continue on reverse side if necessary and identify by block number)

photon counter, speckle imaging

20. ABSTRACT (Continue on reverse side if necessary and identify by block number)

Description is made of two-dimensional photon counters that preserve the temporal ordering of the photons in a form suitable for a new algorithm for speckle imaging. Specifications are given for such a device that is under development by Lockheed and attention is given to a commercially available device that is being procured under this contract. Certain developments concerning the calibration and sensitivity of the speckle imaging algorithm are also described.

DD FORM 1 JAN 73 1473 EDITION OF 1 NOV 65 IS OBSOLETE

UNCLASSIFIED

NOTICE

When Government drawings, specifications, or other data are used for any purpose other than in connection with a definitely related Government procurement operation, the United States Government thereby incurs no responsibility nor any obligation whatsoever; and the fact that the Government may have formulated, furnished, or in any way supplied the said drawings, specifications, or other data, is not to be regarded by implication or otherwise as in any manner licensing the holder or any other person or corporation, or conveying any rights or permission to manufacture, use, or sell any patented invention that may in any way be related thereto.

This technical report has been reviewed and is approved for publication.

_____ _____

FOR THE COMMANDER

_____

INTRODUCTION

The aim of this ongoing project is to implement the new speckle imaging technique proposed in "Speckle imaging, photon by photon" (L. Mertz, 1979, Applied Optics, 18, 611-614; enclosed as Appendix A). Successful speckle imaging would permit much higher resolution images of the sun than are presently available. Such images could then be used for detailed interpretation of the solar magnetic field structure. Our proposed speckle imaging technique is contingent on observational data from a 2-D photon counter that preserves the temporal order of the incident photons, as opposed to the images that are provided by customary observing devices.

PRIOR 2-D PHOTON COUNTERS

For a perspective, the two articles, "Low Light Level Detectors for Astronomy" (P. B. Boyce, 1977, Science, 198, 145-148) and "Detectors for the Space Telescope" (T. Kelsall, 1978, SPIE Proc., 143, 27-35) review the state-of-the-art concerning photon counting image detectors. Those articles describe concern about sensitivity to individual photons as discrete events and there is considerable emphasis on CCD devices, but negligible consideration for preserving the temporal ordering of the photons. Two of the devices discussed in the latter article, the PHOTOCON and the MAMA detectors, indeed, preserve that order. However, neither of those detectors is commercially available or even functioning on a routine observational basis, perhaps, because both include the position discrimination as a special internal part of a microchannel-plate image intensifier tube. The internal part senses the position of the electron bursts emanating as events from the microchannel plate. The internal location of the position sensor requires that the construction effort be delegated to a vendor that is both capable and willing to fabricate the special tube. It also means that the device must function completely satisfactorily at the outset, because adjustments or repairs require breaking the vacuum seal and dismantling the tube.

Rather than hope for the availability of either of those detectors, a more expedient and more cost-effective course seemed to construct a

detector by providing external position sensing of the photon bursts emanating as events from the phosphor screen of an almost standard commercial microchannel plate image intensifier tube.

ANALOG OPTICAL POSITION SENSING DEVICE

For further perspectives relating to the eventual instrument, the simplest arrangement would involve three photomultipliers viewing the phosphor screen of an image intensifier as shown in Figure 1 (where only two of the three photomultipliers are shown). The vignetting screen partially shades one photomultiplier so that the pulse height ratio of the shaded to the unshaded photomultiplier is a measure of the positional coordinate of the event on the phosphor screen. The vignetting screen for the third photomultiplier (not shown) is oriented in the other direction to furnish the second coordinate of the position. Ratiometric analog-to-digital converters would be suitable for those signal measurements. The main difficulty of this basically analog scheme is that 1% precision of position measurement statistically requires at least 10^4 photons registered on each photomultiplier. Considering the quantum efficiency and the collection efficiency of the system, the image intensifier tube probably would need a gain of at least 10^6, which is really high. Other difficulties are that good electronic stability is needed and that fast A-D converters are expensive.

DIGITAL OPTICAL POSITION SENSING DEVICE

Those difficulties led to a completely digital approach, the basic idea being due to Dr. C. Papaliolios. The idea is that multiple images of the phosphor screen should be formed with suitable optics. A bar mask corresponding to one bit of the event position is placed over each of the images along with a photomultiplier. A typical set of masks is shown in Figure 2. An extra photomultiplier with a totally open mask is included so that for a $2^m \times 2^n$ pixel picture, m+n+1 images with masks and photomultipliers are needed. The open photomultiplier senses the occurrence of a photon burst event; coincident pulses at any of the other photomultipliers indicate that their corresponding bits should be ones,

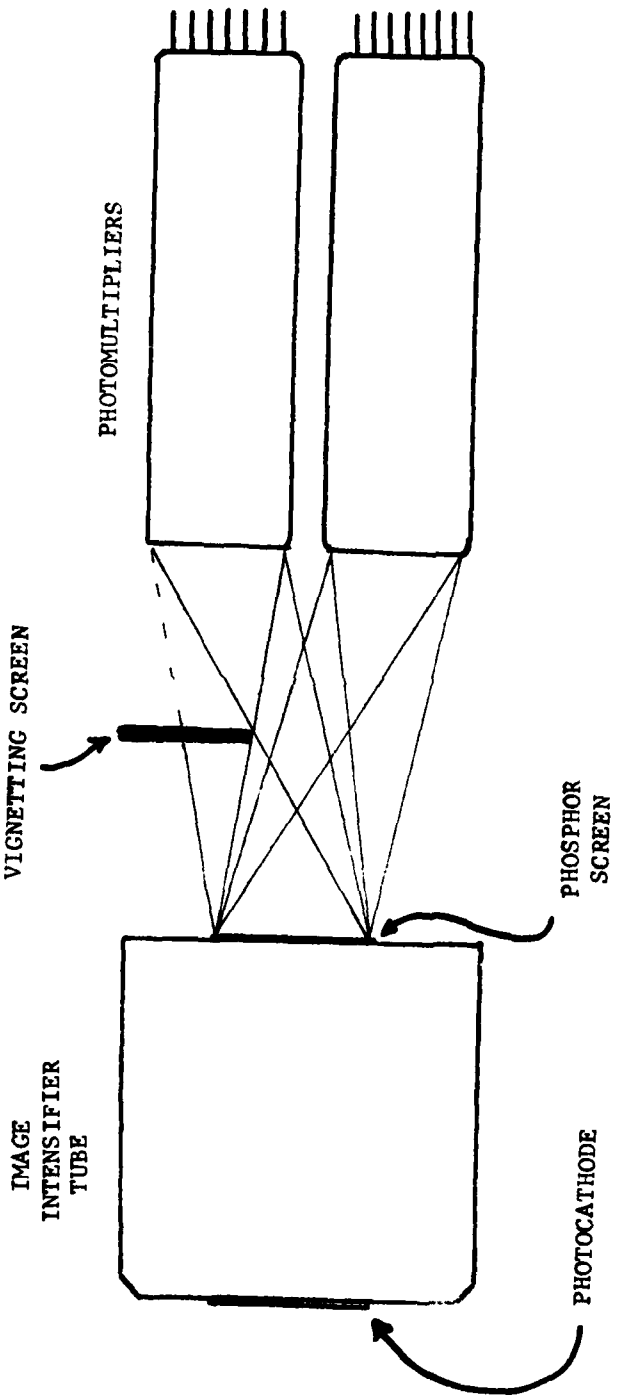

Fig. 1 Photon counter with analog position sensing.

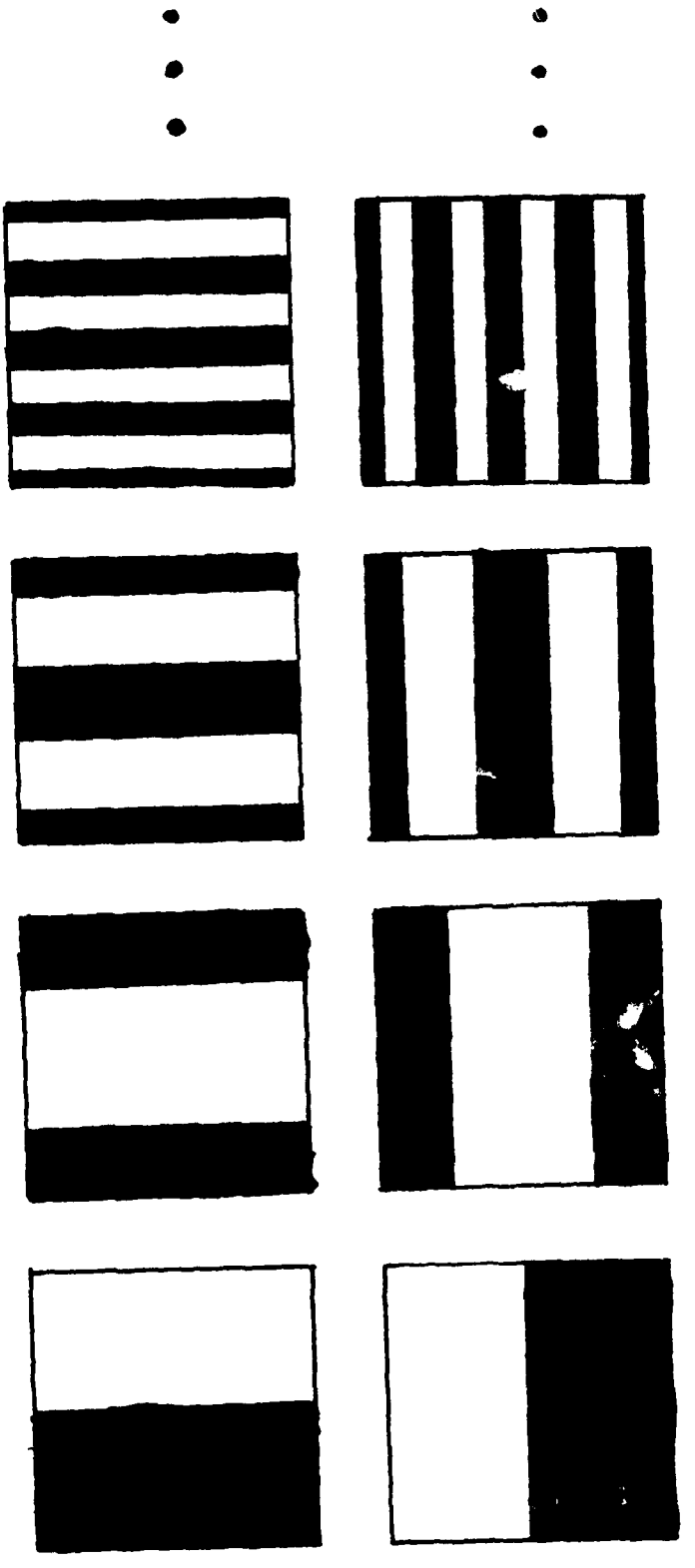

Fig. 2 Bar masks for coding the most significant bits (Gray code).

absence of coincident pulses indicate that their corresponding bits should be zeroes. Thus the positions are immediately in digital form. Incidently, the masks need not be cartesian or even rectangular format. For example, they may be arranged to conform with the s shaped orders of an echelle spectrograph format.

A couple of initial criticisms of the idea were that no centroiding of the photon burst is included to enhance the resolution of the image tube and that it would be mechanically difficult to align the masks and maintain their alignment. In response to the first criticism it should be noted that the binary bar masks should obviously be organized in Gray code. The periodicity of the least significant bit of Gray code happens to be twice that of ordinary binary so that the photon burst may actually be two or even three resolvable pixels in size before the bit loses its significance. In response to the second criticism the multiple images may be obtained with a solid glass prism on which the masks may be firmly glued, thereby assuring stability of their apparent relative positions. That prism also leads to a convenient compact design whose section is shown in Figure 3.

The prism is fabricated by cutting an ordinary right angle prism into pie shaped slices. These slices are cemented together in a circle as they would lie in a complete pie. The masks are glued on as indicated in Figure 4 with the result that the virtual images of the masks are superimposed. The effective glass thickness beneath which the virtual images appear would ordinarily contribute substantial spherical aberration, but that aberration is suppressed by cementing a plano-convec lens on the prism. The lens is chosen so that the virtual images are aplanatically immersed as well as magnified by the refractive index of the glass. The resultant prism is used in conjunction with a transfer lens that gives a real conjugate image of the superimposed virtual images of the masks. The phosphor output screen of the image intensifier is to be located at that real conjugate image. Mask alignment is easily accomplished by viewing and adjusting the registration in the real conjugate image prior to the setting of the glue.

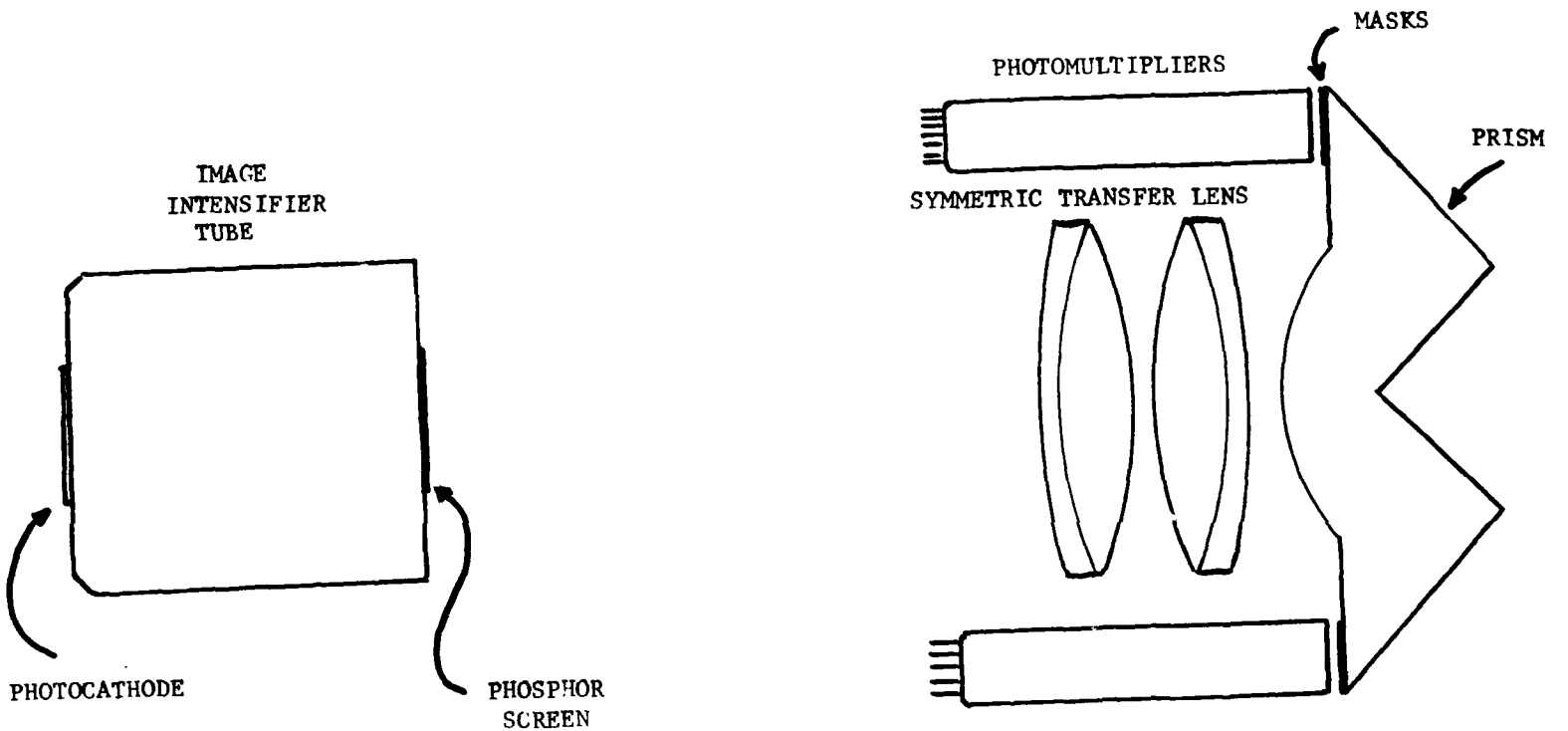

Fig. 3 Photon counter with digital position sensing.

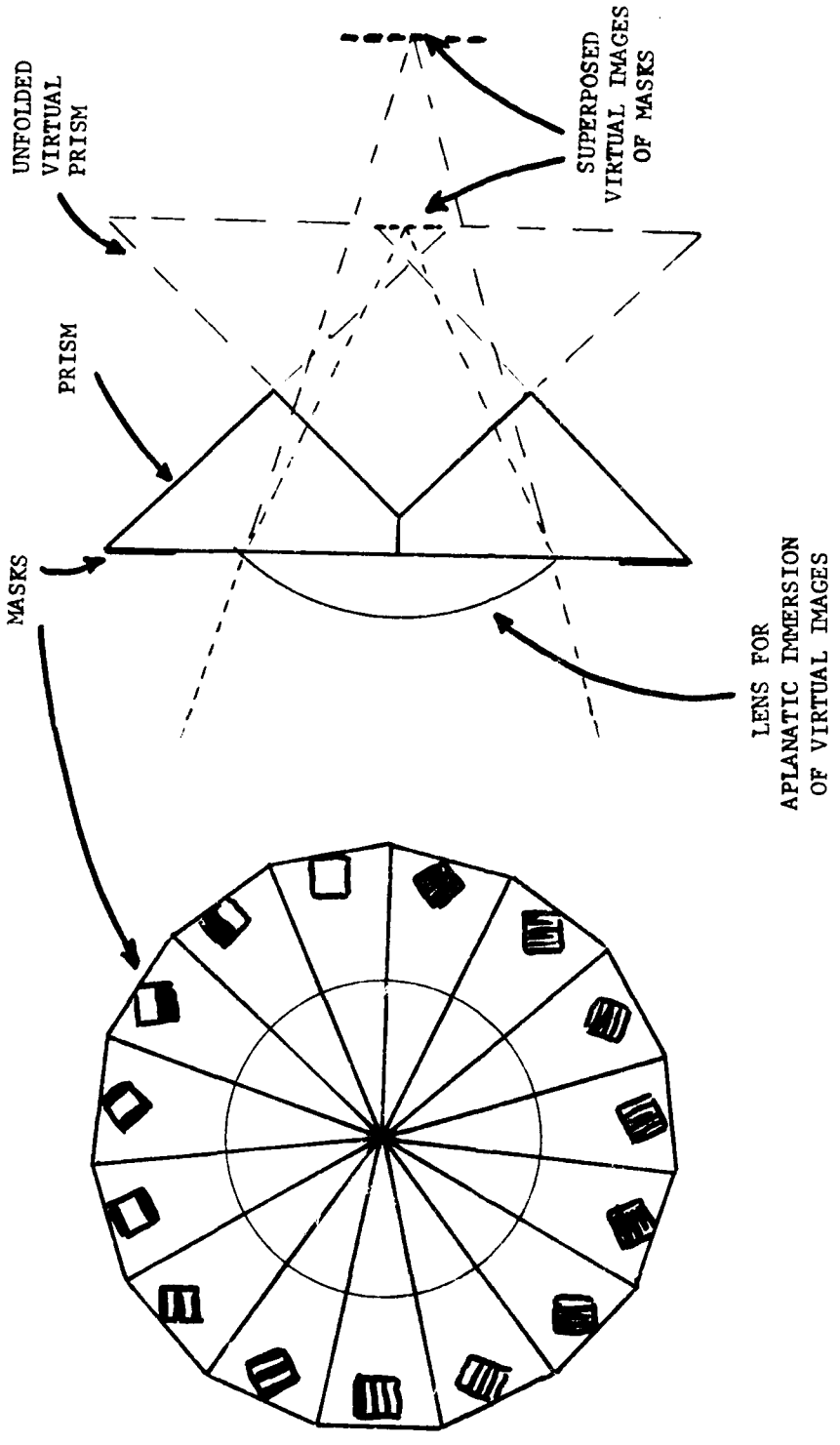

Fig. 4 Prism arrangement

SPECIFICATIONS

The device as constructed employs 15 standard half-inch diameter bialkali photomultipliers to give a 128 x 128 pixel format. Each photomultiplier is followed by a one-transistor emitter follower preamplifier and a high-speed comparator. The comparators each have an adjustable reference threshold and a capacitor feedback to stretch the pulses to about 250 ns. The comparator from the open photomultiplier, after a delay of about 100 ns, initiates a monostable whose leading edge serves as clock to latch the outputs of all the other comparators, thus registering coincidences and non-coincidences. The monostable, whose duration is adjustable, precludes any response to additional pulses during that duration. The latched outputs are then available for digital recording and also go to a Gray to binary analog converter composed of exclusive or gates and thence to digital analog converters, one for each coordinate. The D-A converters are arranged to give 6-bit magnitude and sign so that the analog outputs are bipolar about an origin at the center of the picture format.

The image tube is a standard 2nd generation image intensifier except with a faster phosphor. The model we have is a Varo 3603 with a P22b rather than a P20 phosphor, and its photon bursts are quite readily detectable. The time constant of the phosphor is in the neighborhood of 1 microsecond, even though the decay is not strictly exponential. More recently we had the opoortunity to borrow a Varo 3603 with a P46 phosphor whose output flashes are somewhat shorter with less of an after-tail and roughly 10 times as bright as those of the P22b.

The remaining problem is that the coincidence detection remains unreliable. The causes of the unreliability are not yet identified; they may be sensitivity difficulties, timing difficulties or optical difficulties. As an aid to tracking down the errors, we have constructed an LED (green) flasher that provides 300 ns flashes at 12 microsecond intervals, and the brightness of the flashes is step selectable over the range to emulate the phosphor flashes from the intensifier and up to several times brighter. Of course, the advantage of test flashes for diagnosis is that the location and timing of the flashes is fixed.

COMMERCIALLY AVAILABLE DEVICE

In August 1979, Surface Science Laboratories of Palo Alto announced an imaging electron detector for sale. Their brochure (enclosed, in part, as Appendix B) indicated that a photon sensitive version was under development, simply by placing their electron detector in a vacuum envelope behind a photocathode. Remembering that the aim of our project is speckle imaging rather than detector development, and also in view of the unusual time constraints of the present contract, our most productive course has been to procure the commercial detector. In essence the Surface Science detector is a carefully tailored resistive anode whereby the ratios of discharge distribution among four electrodes specify in analog form the two coordinates of an impinging electron burst. In a sense their device is the electron analog of the simple vignetting photon sensor described earlier, and their device should be subject to similar statistical limitations of precision. They accomplish the requisite high gain by using two microchannel plate electron multipliers in tandem. At any rate, their device functions quite respectably as is evidenced by their demonstrated pictures.

Development of the Lockheed photon counter will nevertheless continue because the direct digital approach offers greater future potential in terms of resolution, speed, dynamic range and format versatility.

SPECKLE IMAGING: AMPLITUDE COMPENSATION

Returning to the topic of the speckle imaging a few theoretical developments have arisen since publication of the Applied Optics article (Appendix A). Dr. T. Tarbell has offered a compelling argument that the amplitudes of the spatial frequency components are necessarily degraded as a result of the image spread. Consider the gedanken experiment of mathematically phase shifting the spatial frequency components of a point image until the point spread function is N times broader (N^2 times larger in area). According to Parseval's theorem the integrated power of the spatial frequencies would remain invariant so that the peak-to-peak speckle amplitudes would diminish by N. That factor is inconsistent

with conservation of energy which requires that the envelope peak diminish by N^2. Consequently the atmospheric spreading must, in fact, degrade the amplitudes of the spatial frequency components, and it will, therefore, be necessary to calibrate and restore the degradation according to

$$A_{corrected} = \frac{A_{measured}}{A_{calibration}} ,$$

where $A_{calibration}$ is the measured amplitude for the spatial frequency component for a source known to be effectively a point. As is well known, when the degradation is severe (small $A_{calibration}$), the large required factor of restoration mainly amplifies noise. Wiener filtering provides a form of compensation that takes noise into account so as to eventually attenuate rather than amplify the diminished amplitudes. Essentially, the form of Wiener filtering is

$$A_{corrected} = \frac{A_{measured} A_{calibration}}{A^2_{calibration} + \sigma^2}$$

where σ is a constant equal to the rms noise present. Asymptotically, when $A_{calibration} >> \sigma$ then the naive restoration formula is followed, but when $A_{calibration} << \sigma$ then the amplitudes are diminished with further decrease in $A_{calibration}$.

Now the speckle imaging algorithm that we are attempting is basically a form of homomorphic signal processing, so that we are concerned and working with the logarithms of the spatial frequency components. While it would be awkward and time consuming to reproduce the Wiener filtering formula in logarithmic form, it is extremely easy to compute the form

$$\log A_{corrected} = \log A_{measured} - \log\sigma - \left|\log A_{calibration} - \log\sigma\right| ,$$

which reproduces the asymptotic behavior of the Wiener filtering formula. Since it is the asymptotic behavior that is most important, this much simplified computing procedure should be perfectly suitable.

SENSITIVITY OF SPECKLE IMAGING

There are also further thoughts concerning the ultimate sensitivity of the technique. In principle the reconstructed picture should be reasonable when the average phase settles to within about a quarter of a turn from the true phase. Suppose that photons arrive at random positions. Applying the algorithm should then lead to a random walk of the phase, and a random walk never settles to a legitimate average. This is in contrast to atmospheric perturbations where shifts must eventually shift back to present a proper average. At the other extreme, when there are lots of photons representing a definite picture and in the absence of atmospheric turbulence, then the phase measurements will be stable. A combination of the extremes such that the random perturbation to the phase never leads to a one-turn slip is still alright for averaging. But if the perturbation should lead to a slip of one cycle in the middle of the observing run, then the phase average will end up in antiphase with the desired average. In other words, at sufficiently low brightness levels or with sufficient sky background, the photon noise perturbations can destroy the validity of the averaging procedure. These notions relating to limiting sensitivity may prove to be tantamount to just another point of view on calculations that others have already made concerning limiting sensitivity of speckle techniques. The additional point of view is still welcome if it can simplify our understanding of the nature of the limiting sensitivity.

Reprinted from **APPLIED OPTICS**, Vol. 18, page 611, March 1, 1979

Speckle imaging, photon by photon

Lawrence N. Mertz

A speckle processing prescription is described that should yield diffraction limited performance for large telescopes in spite of atmospheric turbulence and at light levels as low as 100 photons/sec in the picture. The prescription involves rearranging the spatial frequency components of running glimpses of the scene according to the complex information (entropy) of those components. The imaginary part (phase) of the information is rendered unambiguous by maintaining track of the phase. A 2-D photon counter furnishes the raw observations. Comparisons and ramifications of the procedure are discussed.

Introduction

The goal of this work is to attain diffraction-limited performance for large telescopes in spite of atmospheric turbulence. That possibility has become realistic as the result of Labeyrie's[1] recognition that the atmosphere rearranges rather than obliterates the details of an image. The Abbé perspective that views an image not as an ensemble of pixels but as an ensemble of spatial frequencies is heuristically preferable. Within an isoplanatic field (~3 sec of arc) the predominant effect of atmospheric turbulence is to shift the position (phase) of any individual spatial frequency. The average of a bar pattern (spatial frequency) that is shifting by more than half a bar washes out the contrast of that pattern and is therefore to be avoided. The essence of the algorithm to be described is to average separately the strength and position of the shifting bar patterns.

Detection

The observational raw material for this algorithm is preferably obtained with a 2-D photon counter, which is a device that lists both coordinates of successively arriving photons. Such a list is clearly more informative than an image because the list may be irreversibly transformed to an image. Furthermore, at low light levels the list becomes more efficient than an image because at low light levels most of the capacity of the image is then wasted indicating only the absence of photons. Given the motivation, several elegantly simple schemes for constructing such a device have been devised but will not be described here. Photon rates in the neighborhood of 100–10,000 photons/sec in the entire picture will be considered.

Algorithm

The memory size of the computer shall be four times the number of pixels in the final image. Thus a $16K \times 16$-bit computer will suffice in this example to yield a 64×64 picture ($4K$ pixels). The list of photon coordinates is off line, preferably on magnetic tape. The computer memory shall be divided into eight equal sections of $2K$ words each. The first section will include the program, which is very short, a 320-word table of $1\frac{1}{4}$ cycles of a sine wave, and a stack, called the K stack, of length ranging from 2 to 256 words. This K stack will be used to store the coordinates of photons currently being digested by the computer. The length of the K stack shall be such that all K photons arrive while the atmosphere is essentially static, i.e., within about 1/50 sec.

Each remaining section is to be construed as a 2-D array $A_j(U,V)$, with U ranging from 1 to 32 and V ranging from −31 to +32. These arrays will be initialized to zero. Computations will then commence as follows.

The coordinates (X and Y in packed form) of the first photon are read in to the first word of the K stack. Copying from the sine-cosine table,

$$A_1(U,V) = \cos(XU + YV),$$

$$A_2(U,V) = \sin(XU + YV).$$

Continuing to read in photons until the K stack is full,

$$A_1(U,V) = \sum^{K} \cos(X_k U + Y_k V) = \mathrm{Re}[Z_j(U,V)] = a_j(U,V),$$

$$A_2(U,V) = \sum^{K} \sin(X_k U + Y_k V) = \mathrm{Im}[Z_j(U,V)] = b_j(U,V).$$

The author is with Lockheed Research Laboratory, Palo Alto, California 94304.

Received 14 March 1978
0003-6935/79/050611-04$00.50/0.

At the conclusion of this first filling of the K stack, $t = 1$.

In this fashion we have synthesized the Fourier transform, $Z_t(U,V)$, of the image corresponding to the first K photons of the list, and a few comments are in order. The image is necessarily real, and therefore the Fourier transform is Hermitian, so that only a half plane need be stored. In other words the combined arrays A_1 and A_2 map reversibly to the 64×64 picture.

Second, if K is small this synthesis procedure will be faster than a fast Fourier transform. Moreover, the speed is still greater because no multiplications at all are involved; $(X_k U + Y_k V)$ is obtained from additive recursion, sine-cosine is obtained from table lookup, and the coefficients are all unity because each photon is one unit.

The next task is to ascertain the strength and position of each spatial frequency. Position presents the awkward problem since phase as determined from $\phi = \arctan(b/a)$ is only a partial measure of position. That phase ϕ is only the fractional part of a turn, integral turns being undetermined. Dramatic errors will occur if we attempt to average a set of values knowing only their fractional parts. Therefore, let us establish a complete position Φ that includes integral turns,

$$\Phi_t(U,V) = \Phi_{t-1}(U,V) + [\phi_t - \Phi_{t-1}(U,V)]_{\pm\frac{1}{2}},$$

with $\Phi_0 = 0$. The bracketed expression is reduced to lying between $\pm\frac{1}{2}$ turn by arithmetic left and right shifts, easy computer operations. Basically this procedure tracks the phase by differentiating and integrating so as to follow and keep track of integral turns.

Progression in time occurs as follows. The K stack is full, so we subtract the sine and cosine terms due to the initial photon from $A_{1,2}(U,V)$. That leaves room in the K stack to add the next photon so that we now have at $t = 2$ the Fourier transform of photons 2 to $K + 1$ in place of the previous Fourier transform of photons 1 to K. It is this stage that gives rise to the descriptive phrase: photon by photon. Actually it is permissible to shift by several photons as long as several is appreciably less than K. The new Fourier transform is very redundant with the previous one, and therefore we can be confident that the phases will have shifted by less than half a cycle, so that the phase tracking is legitimate. Furthermore, this recursive progression of the Fourier transform is still faster than starting from scratch because even fewer than K photons are involved.

It is now possible to consider averaging the strength and position of the components so that in the course of the computation we can let

$$A_1(U,V) = \sum_{t=1}^{T} |Z(U,V)|,$$

$$A_2(U,V) = \sum_{t=1}^{T} \Phi(U,V)$$

where $|Z| = (a^2 + b^2)^{1/2} = a\cos\phi + b\sin\phi$.

At the conclusion of exhausting the catalog T, an estimate of an average Fourier transform is available as

$$\text{Est } Z_{U,V} = \frac{1}{T}\sum_{t=1}^{T} |Z| \exp 2\pi i \frac{1}{T}\sum_{t=1}^{T} \Phi = \frac{A_1}{T} \exp 2\pi i \frac{A_2}{T}.$$

By the time the position average settles to within $\frac{1}{4}$ turn accuracy, this estimate may be reconstructed back to a detailed diffraction-limited image by a final conventional 2-D fast Fourier transform.

Comparative Comments

At this stage several comparative comments are in order. The first is a comparison with Labeyrie's speckle interferometry. Speckle interferometry works for centrosymmetric objects. In other words, the Fourier components are all cosinusoidal so that the phases may be specified as zero and need not be ascertained. He uses a power spectrum averaging for the strength of the components. The power spectrum gives slightly different weighting than the amplitude average, but nevertheless the estimate is not grossly different.

The phase-tracking procedure may be also compared with the Knox-Thompson[2] algorithm. The Knox-Thompson algorithm differentiates with respect to spatial frequency, rather than time, for tracking. As a result their procedure can operate with only occasional glimpses of the scene. Fewer calculations are then required under relatively high brightness conditions because temporally contiguous glimpses would be redundant. The Knox-Thompson differentiation procedure uses

$$Z_t Z^*_{t-1} = |Z_t||Z_{t-1}| \exp 2\pi i(\phi_t - \phi_{t-1})$$

The phase difference angle is always less than $\frac{1}{2}$ turn so that the imaginary part of the expression is an amplitude weighted approximation to that difference angle. Also their integration procedure accumulates round-off errors. The tracking difference procedure may be applied equally in spatial frequency with only modest extra calculational effort by

$$\Phi_t = [\phi_t - \Phi_{t-1}]_{\pm\frac{1}{2}} + \Phi_{t-1}, \qquad \Phi_0 = 0.$$

A summary comparison of the estimated phase angles is

$$\text{(A)} \qquad \Phi = \frac{1}{T}\sum_{t=1}^{T}\left[\sum_{\tau=1}^{t}(\phi_\tau - \phi_{\tau-1})\right],$$

where $\phi_{\tau=0} = 0$, and τ is just a dummy index for the temporal integration. For the Knox-Thompson algorithm

$$\text{(B)} \qquad \langle\Phi_{U,V}\rangle = \sum_{t=1}^{N} \arctan\left(\frac{\sum_{t=1}^{T} \text{Im}|Z_t Z^*_{t-1}|}{\sum_{t=1}^{T} \text{Re}|Z_t Z^*_{t-1}|}\right) \qquad (1)$$

$$= \sum_{\tau=1}^{N}\left[\frac{1}{T}\sum_{t=1}^{T}(\phi_\tau - \phi_{\tau-1})\right], \qquad (2)$$

and $\phi_{\tau=0} = 0$. When the phase differences are small, the approximation is close, but I contend that the expression (2) is actually more legitimate than Eq. (1). The establishment of a null border around the picture would serve to diminish the phase difference angles and improve the approximation of Eq. (1). In either case

summation with respect to T before with respect to V is particularly susceptible to accumulated round-off error. Interchanging the summation leads to a possible third version,

$$\langle \Phi_t \rangle = \frac{1}{T} \sum_{t=1}^{T} \left[\sum_{v=1}^{V} (\phi_{t,v} - \phi_{t,v-1}) \right], \tag{C}$$

that should be less susceptible to round-off even though it requires more arithmetic operations.

A third comment relates to the length of the K stack. As stated previously, K should be no longer than the coherence time of the atmosphere, in other words less than a half cycle of the highest really significant fluctuation frequency. That time depends somewhat on atmospheric conditions but is typically about 1/50 sec. At the other extreme how short may K be? The answer is 2, because if K were to be only 1, the reconstructed picture would consist of a single point at the mean photon arrival position.

A fourth comment relates to the susceptibility of all these algorithms to telescope aberrations, particularly to nonsymmetric aberrations. Consider at first a nonturbulent or static atmosphere. Except for photon statistics, all glimpses of the picture are then identical, and the averaging simply reconstructs that same picture, which includes telescope aberrations. If we now let the atmosphere become gradually more turbulent, more variance of Φ develops, but the average still centers around the systematic value of Φ given by the telescope aberrated picture. Therefore, I contend that these speckle imaging procedures give the telescope aberrated picture rather than an unadulterated diffraction-limited picture. On the other hand, it should not be difficult to calibrate the aberrations by observing an unresolved star and subtracting the systematic Φ of the aberrations from those of the unknown picture to obtain an unaberrated diffraction-limited picture. $A_7(U,V)$ is reserved for storage of the reference Φ_{ref}. Such calibration requires only that the telescope aberrations be reproducible.

Improvements

Let us now return toward improving the estimate of the algorithm. The atmospheric effect of shifting the complex Fourier components is mathematically multiplicative. There is a less severe, but nevertheless appreciable, effect on the Fourier amplitudes that also is a multiplicative process and must be averaged out. It should be preferable, however, to have an additive process so that the fluctuating component may have a proper zero mean. The requisite process conversion is accomplished simply by taking logarithms of the complex Fourier components, a procedure that is used in cepstral analysis[3] for use with homomorphic signal processing, of which this speckle imaging may be a 2-D example. If Z is complex, $\ln Z$ is complex;

$$Z = a + ib = \exp(\ln Z) = \exp(\alpha + i\beta).$$

We note that $\alpha = \ln|Z|$ and $\beta = 2\pi\Phi$, so that it should be preferable to calculate

$$A_4(U,V) = \sum_{t=1}^{T} \ln|Z_t|$$

and use the estimate

$$\text{Est}(Z) = \exp\left(\frac{1}{T}\sum_{t=1}^{T} \ln Z_t\right) = \exp\frac{1}{T}(A_4 + 2\pi i A_5)$$

A further improvement may be available by noting that if the amplitude of a Fourier component happens to be strong, there will be less uncertainty in the determination of its position. Thus an amplitude weighting is desirable for the position average, and not to discriminate against the real part, that also should be weighted. Thus we should calculate

$$A_4(U,V) = \sum_{t=1}^{T} |Z_t| \ln|Z_t|,$$

$$A_5(U,V) = \sum_{t=1}^{T} |Z_t|\Phi_t,$$

$$A_6(U,V) = \sum_{t=1}^{T} |Z_t|,$$

and use the estimate

$$\text{Est}(Z) = \exp\frac{\sum|Z|\ln Z}{\sum|Z|} = \exp\frac{1}{A_6}(A_4 + 2\pi i A_5),$$

as the basis for reconstructing the picture. Note that the entropy form of the expression has entered in a very natural way. Insofar as entropy is identified with probabilistic information, I suspect that the picture based on this last estimate is the most probable picture, in a Bayesian sense, that would have given rise to the observed photon catalog.

Speed

For a minicomputer using software multiply the conversion from rectangular (a,b) to polar $(|Z|,\phi)$ notation, and the logarithmic function takes much more time than the synthesis of the Fourier transforms. For the 64×64 scale of the example the program runs about 500 times slower than real time, so that 10 sec of data would require about 1½ h of computation. That rate is not at all discouraging, and much faster rates (even real time for TV size pictures) may be anticipated eventually because the algorithm is so suitable for mixed parallel-serial processing.

The attainment of diffraction-limited resolving power in the Rayleigh sense means that the spatial frequencies are each correctly positioned to within about ¼ bar (fringe). Thus if the rms atmospheric phase perturbation is five fringes we may expect to need about $20^2 = 400$ statistically independent samples for their average to settle within that Rayleigh criterion. Presuming that samples separated by about 1/10 sec are fairly independent, about 40 sec of observation should be sufficient to quell the effects of atmospheric turbulence.

Noise

Let us now examine the behavior of speckle imaging with respect to noise. One principal task of a large telescope is to seek ever fainter stars. The obstacle is the background illumination from the night sky, so that the function of the telescope is not only to gather pho-

tons but also to isolate the stellar photons as thoroughly as possible from the night sky photons. Superior isolation is in fact one major goal of the space telescope. For speckle imaging a uniform background, along with its statistical fluctuations, gets rearranged into a uniform background with comparable statistical fluctuations. A star, on the other hand, gets rearranged from an extended patch to a concentrated point. Therefore, the contrast of the star to background should be augmented highly, accomplishing from the ground that major goal of the space telescope.

The repercussions with respect to very large telescopes should also be important. The motivation toward larger apertures should now be enhanced by the new opportunity to increase resolving power as well as collecting area. Economy dictates that very large apertures be assembled from pieces with the result that random aberrations will be much larger than the diffraction limit even though the quality commensurate with atmospheric seeing is attained. However, those aberrations must be reproducible if they are to be removed by calibration. The motions of any assembly of servo-controlled pieces will certainly hinder greatly, and probably rule out completely, this use of speckle imaging to gain the diffraction limit. It is far more likely that an immobile aperture, such as the Arecibo concept that I have long advocated,[4] might succeed. A very narrowband (~1-Å) color filter would permit operation independent of primitive phasing (piston) errors of the pieces. It should be remembered that the decrease in flux by the restriction to narrow bandwidth also applies to the night sky and furthermore would be compensated by the enormous collecting area of the aperture.

Remarks

It is a pleasure to call attention to a commendably clear and thorough review article by Worden[5] describing previous work in speckle imaging. The present work originated while I was at the Smithsonian Astrophysical Observatory; ordinarily publication should have been deferred pending experimental verification. However, the necessary experiments have had to be adjourned since I am no longer employed there. Nevertheless the goal of attaining diffraction-limited performance for large telescopes seems so worthwhile and so accessible that I still hope for the opportunity to resurrect the experimental work.

Postscript. Thanks to my new employer, this speckle project is being started afresh.

References

1. A. Labeyrie, Astron. Astrophys. **6**, 85 (1970).
2. K. T. Knox and B. J. Thompson, Astrophys. J. **193**, L45 (1974).
3. D. G. Childers, D. P. Skinner, and R. C. Kemerait, Proc. IEEE **65**, 1428 (1977).
4. L. Mertz, in *Optical Instruments and Techniques*, J. Home Dickson, Ed. (Oriel, London, 1970), p. 507.
5. S. P. Worden, Vistas Astron. **20**, 301 (1977).

JUST ONE electron/msec ... HONEST.

That's the illumination we used to take this picture

With our unique

IMAGING PARTICLE DETECTOR

Each dot on this CRT photo represents a single electron passing through an object mask onto our detector (30 sec exposure)

USES

- Detector for electron spectrometers; mass spectrometers; UV/X-Ray imaging systems; particle physics experiments etc

FEATURES

- High total quantum efficiency
- Useful in fluxes up to 10^5 events/sec dead time 7μsec
- Excellent spatial resolution (>100 line pairs/in
- Compact: 2" Dia., 1.5" thick including electron multipliers.
- Extremely rugged, stable, and long-lived
- Digital or analog outputs available

HOW IT WORKS

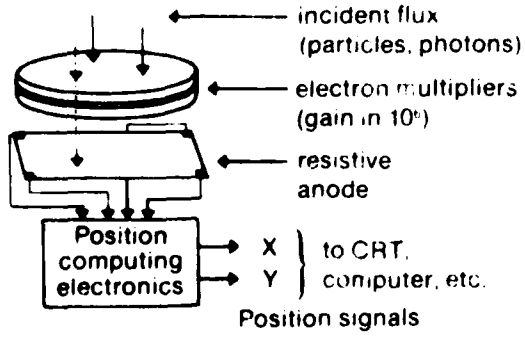

- A particle strikes the electron multipliers producing a pulse of 10^6 electrons.
- This charge is collected by 4 electrodes on a resistive anode.
- The (x,y) position of the particle is computed from the charge division among the electrodes.

Call Mike Kelly at

SURFACE SCIENCE LABORATORIES
4151 Middlefield Road
Palo Alto, CA 94303
415 493-0229

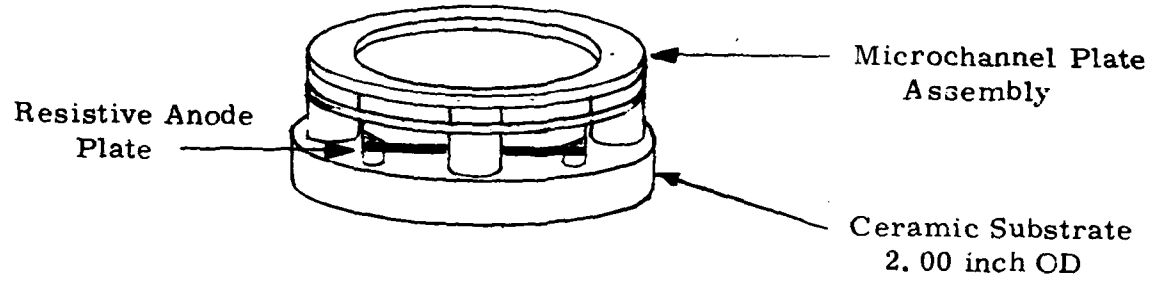

Figure 1.5

Physical Configuration of
Detector Assembly.

The two microchannel plates are supported over the resistive anode by gold plated stainless steel rings, and held in place by spring-loaded contacts. All bias and signal connections are made to pins on the underside of the ceramic base plate. Signal leads are capacitively decoupled, so the detector can be biased with respect to ground. The overall height of the detector (including the decoupling network mounted on the ceramic plate) is approximately one inch. The unit can be mounted from the front or rear as desired, using mounting holes provided. It is made entirely of high vacuum compatible materials and can be baked to 300°C.

PERFORMANCE

The two photographs on the next page show the performance of the overall two-dimensional system. They are photos of a storage scope connected to the "X" and "Y" outputs of the electronic unit. The input of the two microchannel plates was covered by a mask having the test pattern on it and illuminated by a source of electrons.

Performance of Two-Dimensional Resistive Anode Detector

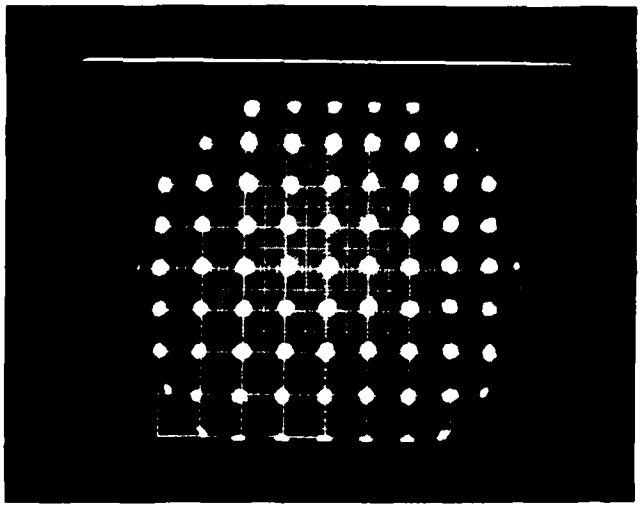

Figure 1.3 Example of detector linearity: electron image of shadow mask with 0.1 inch hole spacing.

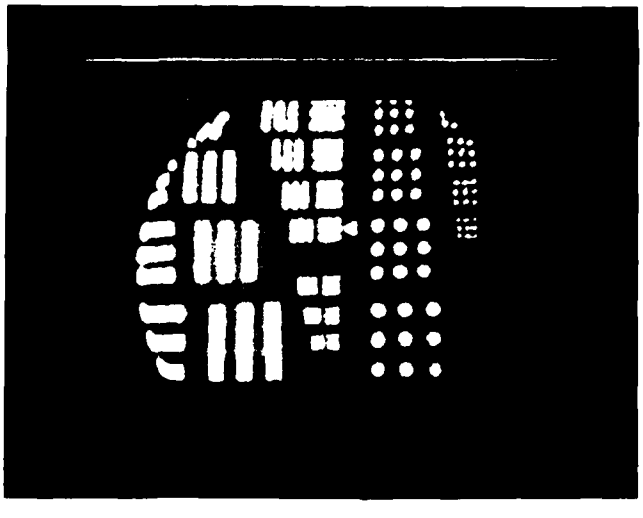

Figure 1.4 Example of detector resolution: image size is 0.1 inch/division.

Optical Detectors

To use the imaging detector for visible radiation, a photocathode must be added as shown in the figure below. SSL does not at present have such a configuration available, but one is under development.

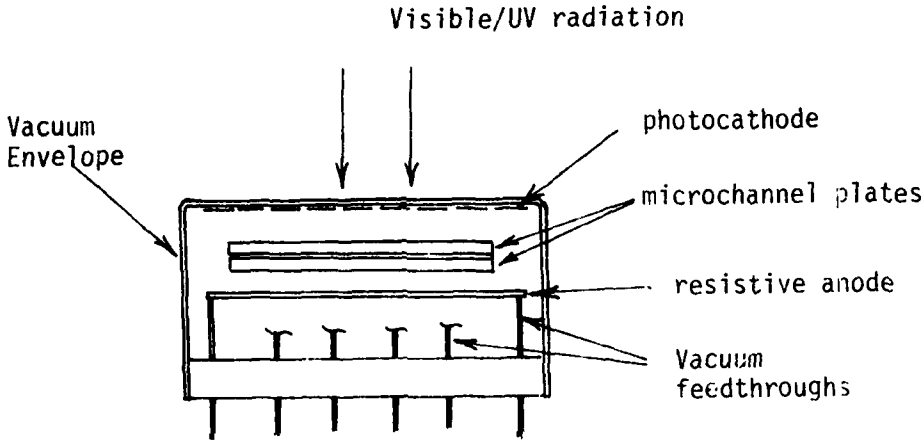

For further details please contact Mike Kelly at Surface Science Laboratories